國立臺灣大學電機資訊學院資訊工程研究所

碩士論文

Graduate Institute of Applied Physics
College of Science
National Taiwan University

Master Thesis

中文標題，請到ntuvars.tex輸入你的資料

English title MsWave

王瑞斌
Jui-Pin Wang

指導教授：林守德博士
Advisor: Shou-De Lin, Ph.D.

中華民國 102 年 7 月
July, 2013

國立臺灣大學
資訊工程研究所

碩士論文

中文標題，請到ntuvars.tex輸入你的資料

王瑞斌 撰

1027

國立臺灣大學（碩）博士學位論文
口試委員會審定書

論文中文題目

論文英文題目

本論文係○○○君（○學號○）在國立臺灣大學○○學系、所完成之碩（博）士學位論文，於民國○○年○○月○○日承下列考試委員審查通過及口試及格，特此證明

口試委員：

（簽名）

（指導教授）

系主任、所長 （簽名）

（是否須簽章依各院系所規定）

致謝

這裡將簡單介紹如何利用 LaTeX 來編輯你的畢業論文，若不知道 LaTeX 是什麼或是沒有概念的話，建議你可以簡單看過放在此資料夾裡的李果正 -大家來學 LaTeX前四章內容，在下載適合的 LaTeX 整合發行套件之後（請看第 III.項），可以嘗試用剛安裝好的 LaTeX 編輯器來編譯thesis.tex這份文件，編譯的方法可以看下面第 V.項的介紹，若編譯成功，所編譯出來的 thesis.pdf 文件的應該會跟此 demo.pdf 文件一模一樣，而且沒有任何問號符號，走到這一步的話，就差不多可以開始邊學習 LaTeX 邊編輯你的畢業論文了！基本上會使用到的指令都包含在論文的的各章節裡，怎麼在論文裡寫公式或是放圖之類的就自行看 tex 檔學吧。如果有任何問題或建議可以來信與我討論，我的信箱是dran31545@gmail.com，或是到此範本Google Project裡面的Issues貼上你的問題與建議，我會盡我所能更新此範本，也歡迎大家自行重製、改良此範本並散布給他人，祝大家順利畢業！

要編輯致謝請打開acknowledgementsCH.tex

I. 此範本參考並修改自下列網站的資料：

- 如何用 LaTeX 排版臺灣大學碩士論文
  —台灣大學論文 LaTeX 樣版原創者黃子桓的教學網頁
- LaTeX 常用語法及論文範本
  —Hitripod所修改的範本，這裡參考了許多他所寫的格式和內容
- 使用 LaTeX 做出精美的論文
- XeTeX：解決 LaTeX 惱人的中文字型問題
- 台灣大學碩士、博士論文的 Latex 模板

II. 幾個有用的參考資料及網路資源：

- 李果正 -大家來學 LaTeX—建議先看完前四章
- WIKIBOOKS-LaTeX—好用的線上工具書
- Working with a .bib file using JabRef
- Using BibDesk - A short tutorial
- LaTeX for Physicists

III. 下載 LaTeX 整合發行套件，可參考TeX Collection：

1. MacTeX: For **MacOSX**，下載MacTeX.pkg
2. ProTeXt: For **Windows**，下載ISO file
3. TeX Live: For **GNU/Linux** and **MacOSX**, and **Windows**，下載ISO file
4. CTAN: The Comprehensive TeX Archive Network.

IV. 好用的程式：

- 文獻管理系統：
  1. JabRef
     可參考Working with a .bib file using JabRef或是Google及YouTube
  2. BibDesk (For Mac)
     可參考Using BibDesk - A short tutorial或是Google及YouTube
- 方程式編輯器：Daum Equation Editor (Chrome App，必須使用 Google 瀏覽器)

V. 編譯流程：

1. `xelatex thesis`
   對 thesis.tex 進行第一次 XeLaTeX 編譯，產生 thesis.pdf 以其他檔案
2. `bibtex thesis`
   對 thesis.tex 進行 BibTeX 編譯，產生 bbl 檔以及 blg 檔
3. `xelatex thesis`
   對 thesis.tex 進行第二次 XeLaTeX 編譯，產生目錄、圖表連結及參考文獻
4. `xelatex thesis`
   對 thesis.tex 進行第三次 XeLaTeX 編譯，產生參考文獻連結，完成編譯

注意！此範本使用 cite 套件，可依據你利用文獻管理系統所整理好的thesisbib.bib檔在論文最後產生參考文獻頁面，若你的系所規定要在每個章節的後面產生參考文獻，則可以用 chapterbib 套件，來對每個有附參考文獻的章節 tex 檔進行一次 BibTeX 編譯產生 bbl 檔，如範例的introduction.tex、THM.tex和EXP.tex，如果有這需要請把thesis.tex檔裡使用 cite 套件的指令利用註解符號% 來取消使用 cite 套件，並刪去出現在使用 chapterbib 套件指令前面的註解符號% 來啟動使用 chapterbib 套件

```
\usepackage{cite}
%\usepackage{chapterbib}
```

改成

```
%\usepackage{cite}
\usepackage{chapterbib}
```

再來利用註解符號% 取消會把參考文獻放在論文最後的指令

```
\bibliographystyle{unsrt}
\addcontentsline{toc}{chapter}{\bibname}
\bibliography{thesisbib}
```

改成

```
%\bibliographystyle{unsrt}
%\addcontentsline{toc}{chapter}{\bibname}
%\bibliography{thesisbib}
```

再把用來輸入章節檔案的 \input 指令改成 \include 指令

```
\input{introduction}   =>   \include{introduction}
\input{THM}            =>   \include{THM}
\input{EXP}            =>   \include{EXP}
```

最後記得在每個有附參考文獻的章節加上產生參考文獻的指令，即在introduction.tex、THM.tex和EXP.tex三個檔案裡最後啟動下面兩行指令

```
%\bibliographystyle{unsrt} => \bibliographystyle{unsrt}
%\bibliography{thesisbib}  =>  \bibliography{thesisbib}
```

而編譯時則需要對有附參考文獻的introduction.tex、THM.tex和EXP.tex各做一次 BibTeX 編譯，編譯流程如下

1. `xelatex thesis`
   對 thesis.tex 進行第一次 XeLaTeX 編譯，產生 thesis.pdf 及其他檔案
2. `bibtex introduction`
   對 introduction.tex 進行 BibTeX 編譯，產生 bbl 檔以及 blg 檔
3. `bibtex THM`
   對 THM.tex 進行 BibTeX 編譯，產生 bbl 檔以及 blg 檔
4. `bibtex EXP`
   對 EXP.tex 進行 BibTeX 編譯，產生 bbl 檔以及 blg 檔
5. `xelatex thesis`
   對 thesis.tex 進行第二次 XeLaTeX 編譯，產生目錄、圖表連結及參考文獻

6. `xelatex thesis`
   對 thesis.tex 進行第三次 XeLaTeX 編譯，產生參考文獻連結，完成編譯

VI. 補充說明與注意事項：

- 口試委員會審定書：
  請到台大圖書館網頁的電子論文服務下載論文格式範本，並修改成正確的格式，也可到此範本所在資料夾的cert.doc修改。當然你也可以利用 LaTeX 來編輯，你只要填好ntuvars.tex檔的資料，並去除在 thesis.tex 裡下面這行的註解符號%

  ```
  %\makecertification
  ```

  編譯完後就可以產生審定書格式。口試通過後，請把已經簽名的審定書掃描成 pdf 檔，再取代原本的cert.pdf，即可放上已簽名的審定書。處理審定書出現的指令在 thesis.tex 裡

  ```
  %----------- generate the certification ...
  %\makecertification
  %----------- includepdf by using package ...
  \addcontentsline{toc}{chapter}{口試委員會審定書}
  \includepdf[pages={1}]{cert.pdf}
  ```

- 浮水印：
  資料夾已經附上浮水印檔案了，若學校有更改，到請到台大圖書館網頁的電子論文服務下載pdf 格式的浮水印到此範本所在資料夾。若要開啟關閉浮水印功能，即自行刪去或加上下面位於thesis.tex指令的註解符號%

  ```
  %\CenterWallPaper{0.174}{watermark.pdf}
  %\setlength{\wpXoffset}{6.1725cm}
  %\setlength{\wpYoffset}{10.5225cm}
  ```

- 單面印刷與雙面印刷：
  此範本為單面印刷，若論文頁數超過 80 頁，依規定需要用雙面印刷，此時只需把 thesis.tex 裡的

  ```
  \documentclass[a4paper, 12pt, oneside]{book}
  ```

  改成

  ```
  \documentclass[a4paper, 12pt, twoside]{book}
  ```

- 如何加入附錄?

在thesis.tex裡，依需求選擇 input 或 include，刪去% 符號來輸入附錄章節

```
%----------- Input your appendix here  -----------
%\input{AppendixA}
%or %chapter cite  == \include
%\include{AppendixA}
```

在章節檔 AppendixA.tex 裡，開頭打

```
\chapter{First appendix title}
```

即可，以此類推。

- 系上規定論文圖表須全部放到最後獨立出來的章節，且章節不出現在目錄中：
  在thesis.tex裡，依需求選擇 input 或 include，刪去% 符號來輸入圖表章節

```
%----------- Input your Figure chapter here  -----------
%\input{EndFigTab}
%chapter cite  == \include
%\include{EndFigTab}
```

在章節檔EndFigTab.tex裡有範例和說明可供參考，要注意正文的圖表和附錄的圖表要分清楚，即在EndFigTab.tex內

```
\renewcommand{\thefigure}{\arabic{chapter}.
\arabic{figure}}
\renewcommand{\thetable}{\arabic{chapter}.
\arabic{table}}
%--- Input your main figures and tables here  ---
```

這幾行之後章節計數器格式已切換為 1...9，放正文的圖表，

```
\renewcommand{\thefigure}{\Alph{chapter}.
\arabic{figure}}
\renewcommand{\thetable}{\Alph{chapter}.
\arabic{table}}
%--- Input your appendix figures and tables here  ---
```

這幾行之後章節計數器格式已切換為A...Z，放附錄的圖表。另外要取消圖表的浮動功能，才能讓圖表按照指令出現順序排好，即把平常使用的圖表指令

```
\begin{figure}[htb]
...
\begin{table}[htb]
```

改成

```
\begin{figure}[!]
...
\begin{table}[!]
```

剩下的只要注意章節圖表的計數器設定即可。`\ref` 和 `\label` 指令可以在此圖表章節與正文章節使用。

- 如果我想要修改 margin(文字邊界) 的話，可以從哪裡下手呢?
  請打開ntu.sty修改下面這行的上下左右參數即可：

```
\RequirePackage[top=3cm,left=3cm,bottom=2cm,right=3cm]
{geometry}
```

- 我想引用 Twomey (1974): Pollution and planetary albedo 這篇論文，如何用 `\cite` 引用它的時候在內文顯示 Twomey (1974) [編號] ？
  建議使用 natbib 套件，參考資料如下：
  LaTeX/Bibliography Management
  Overview of Bibtex-Styles
  Reference sheet for natbib usage
- XeTeX ：
  此範本中文字體使用XeTeX 轉換，細節請參考Hitripod寫的XeTeX：解決 LaTeX 惱人的中文字型問題。
- 如何輸入英文 ‘單引號’ 和 “雙引號” 以及不同長度的破折號？
  可以參考李果正 -大家來學 LaTeX第 17 頁針對標點符號的遊戲規則，範例如下，輸入以下指令：

```
`單引號'\\
``雙引號''\\
-hyphen\\
--en-dash\\
---em-dash\\
```

則顯示：
‘單引號’
“雙引號”

-hyphen
–en-dash
—em-dash

中文摘要

請打開並編輯abstractCH.tex

關鍵字：壹、貳、參、肆、伍、陸、柒

Abstract

Open and edit abstractEN.tex

Key words:A, B, C, D, E, F, G

Contents

口試委員會審定書 **i**

致謝 **ii**

中文摘要 **ix**

Abstract **x**

Contents **xi**

List of Figures **xiii**

List of Tables **xiv**

1 Get started with LaTeX **1**

1.1 LaTeX Adavanced Features 1

1.1.1 Figure 2

1.1.2 Table 2

1.1.3 Verb 4

1.1.4 Enumeration 4

1.1.5 Code Display 4

1.1.6 Math 5

1.1.7 Algorithms 6

2 Introduction **7**

3 Quantity modulation **8**

3.1 Introduction 8

3.2 System model 9

3.2.1 Transmitter 9

3.2.2 Receiver 9

3.2.3 Channel 10

3.2.4 QM system 11

3.3 Detection in one-shot transmission 12

3.3.1 Binary Detection 12

3.3.2 M-ary Detection 14

3.3.3 Error Rate Analysis 15

3.4 Serial transmision and ISI cancellation 16

3.5 Numerical results 18

3.5.1 SER comparison with and without ISI cancellation 18

3.5.2 Performance Under Different Duration of Time Slot 19

4 Theory of surface plasmon polaritons in metallic nano-structures **21**

4.1 Definition of plasmon 21

4.2 Surface plasmon polaritons at interface between dielectric and metal . . . 23

5 Experiment **26**

5.1 Atomic force microscopy 26

5.2 Scanning electron microscopy 30

Bibliography **33**

List of Figures

1.1 A picture of a tiger. 2

3.1 Transmission from TN to RN through a fluid medium. 10

3.2 Illustration of quantity-based modulation scheme with $L_0 = 2$, $L_1 = 4$, $L_2 = 6$, $L_3 = 8$. 11

3.3 Demonstration of the process of finding η in a binary QM system, where f is the conditional pdf of N given H_m is true. 14

3.4 Theoretical result versus numerical result for one-shot binary quantity-based modulation. 16

3.5 Binary quantity-based modulation with ISI cancellation. 19

3.6 Quaternary quantity-based modulation with ISI cancellation. 20

3.7 Binary quantity-based modulation with ISI cancellation under different T_s. 20

4.1 Longitudinal collective oscillations of the conduction electrons of a metal (Volume plasmons) 21

4.2 Dispersion relation of SPPs at the interface between a Drude metal with negligible collision frequency and air (blue curves) and silica (red curves). 24

4.3 Phase-matching of light to SPPs the grating coupling configuration. . . . 25

5.1 Schematic of atomic force microscopy. 26

5.2 Schematic of optical system for cantilever deflections detection. 27

5.3 Sketch of tip-sample forces. 28

5.4 Basic construction of a scanning electron microscopy. 31

List of Tables

1.1 Table Example 1 2
1.2 Table Example 2 2
1.3 Table Example 3 3
1.4 Table Example 4 3
1.5 Table Example 5 3

Chapter 1

Get started with LaTeX

Three common font styles in this text:

- **Item1**: *Italic 中文 123*
- **Item2**: **Bold 中文 123**
- **Item3**: *slant 中文 123*

About the advance latex grammer see the next section 1.1.

1.1 LaTeX Adavanced Features

The following features would be introduced in the coming subsections:

- SubSection 1.1.1: **Figure**
- SubSection 1.1.3: **Verb**
- SubSection 1.1.3: **Verb**
- SubSection 1.1.4: **Enumeration**
- SubSection 1.1.2: **Table**
- SubSection 1.1.5: **Code Display**
- SubSection 1.1.6: **Math**

- SubSection 1.1.7: **Algorithms**

1.1.1 Figure

Figure 1.1: A picture of a tiger.

Figure 1.1 is a picture of a tiger.

1.1.2 Table

Table examples on WIKIBOOKS.

Table 1.1: Table Example 1

Start	End	Character Block Name
3400	4DB5	CJK Unified Ideographs Extension A
4E00	9FFF	CJK Unified Ideographs

Table 1.2: Table Example 2

Item		
Animal	Description	Price ($)
Gnat	per gram	13.65
	each	0.01
Gnu	stuffed	92.50
Emu	stuffed	33.33
Armadillo	frozen	8.99

Table 1.3: Table Example 3

Allocation	Allocation, Element, Type, Script
Data Types	Byte2, Byte3, and Byte4 Float2, Float3, Float4 Int2, Int3, Int4 Long2, Long3, Long4 Matrix2f, Matrix3f, Matrix4f Short2, Short3, Short4
Graphics	Mesh ProgramFragment, ProgramRaster ProgramStore, ProgramVertex RSSurfaceView

Table 1.4: Table Example 4

Team sheet		
Goalkeeper	GK	Paul Robinson
Defenders	LB	Lucus Radebe
	DC	Michael Duberry
	DC	Dominic Matteo
	RB	Didier Domi
Midfielders	MC	David Batty
	MC	Eirik Bakke
	MC	Jody Morris
Forward	FW	Jamie McMaster
Strikers	ST	Alan Smith
	ST	Mark Viduka

Table 1.5: Table Example 5

Team	P	W	D	L	F	A	Pts
Manchester United	6	4	0	2	10	5	12
Celtic	6	3	0	3	8	9	9
Benfica	6	2	1	3	7	8	7
FC Copenhagen	6	2	1	2	5	8	7

1.1.3 Verb

Let's take a overview on how to type special characters:

`<FRAMEWORKS_BASE>/graphics/java/android/renderscript`

[1] You could also go back to the beginning of the chapter by the **hyperref**.

1.1.4 Enumeration

1. Enumerated Item1
2. Enumerated Item2
3. Enumerated Item3

1.1.5 Code Display

Here is a "Hello, DanDing." example:

```
void main(int argc, char **argv)
{
    printf(" ´  _> `  ");
}
```

Another example with line numbers:

```
1 void main(int argc, char **argv)
2 {
3     printf(" ´  _> `  ");
4 }
```

Matlab example:

```
1 function y = demo(x) % This is a comment.
2     str = 'hello there';
3     y = x + 1;
4 end
```

[1] Path of <APP_intermediates>: <ANDROID_ROOT>/ out/ target/ common/ obj/ APPS/ APP-NAME_intermediates/

1.1.6 Math

- Inline mode:

  The solution to $\sqrt{x} = 5$ is $x = 25$.

- Display mode:

  The solution to

  $$\sqrt{x} = 5$$

  is

  $$x = 25.$$

- Numbered mode:

  $$2 + 2 = 4 \tag{1.1}$$

- Non-numbered:

  $$2 + 2 = 4$$

- Aligning:

  $$\begin{aligned} 2x^2 + 3(x-1)(x-2) &= 2x^2 + 3(x^2 - 3x + 2) \\ &= 2x^2 + 3x^2 - 9x + 6 \\ &= 5x^2 - 9x + 6 \end{aligned}$$

- Fractions:

  $$\frac{n!}{k!(n-k)!} = \binom{n}{k}$$

- Matrix:

  $$A_{m,n} = \begin{pmatrix} a_{1,1} & a_{1,2} & \cdots & a_{1,n} \\ a_{2,1} & a_{2,2} & \cdots & a_{2,n} \\ \vdots & \vdots & \ddots & \vdots \\ a_{m,1} & a_{m,2} & \cdots & a_{m,n} \end{pmatrix}$$

More examples on WIKIBOOKS.

1.1.7 Algorithms

Algorithm 1 Calculate $y = x^n$

Require: $n \geq 0 \vee x \neq 0$
Ensure: $y = x^n$
  $y \Leftarrow 1$
  if $n < 0$ **then**
    $X \Leftarrow 1/x$
    $N \Leftarrow -n$
  else
    $X \Leftarrow x$
    $N \Leftarrow n$
  end if
  while $N \neq 0$ **do**
    if N is even **then**
      $X \Leftarrow X \times X$
      $N \Leftarrow N/2$
    else[N is odd]
      $y \Leftarrow y \times X$
      $N \Leftarrow N - 1$
    end if
  end while

More examples on WIKIBOOKS.

Chapter 2

Introduction

HiHi Iam r44 The organization of this thesis is as follows. In chapte 4, the theoretical background and definition of surface plasmon will be included [1]. Chapte 5 contains description of experiment methods such as atomic force microscopy and scanning electron microscopy.

Chapter 3

Quantity modulation

3.1 Introduction

In this chapter, we study the communication between two nano-machines with information embedded in different molecular quantity [**?**]. In the rest of this chapter, we call this kind of modulation as quantity modulation (QM). It is known that in diffusion-based molecular communications, molecules are emitted by the transmitter and move towards the receiver following the laws of molecule diffusion. Recent studies on diffusion-based molecular communications often model the statistical behavior of molecule diffusion as a Brownian motion [**?**]. Due to the random nature of Brownian motions, molecules that released earlier by TN may arrive late. Therefore, messages carried in current molecules may be interfered by those delayed molecules that were transmitted earlier. This phenomenon is known as the ISI effect in diffusion-based molecular communications. A brief discussion about this effect can be found in [**?**] and [**?**].

There are lots of ways to design filters to eliminate the effect of ISI in conventional communication such as linear equalizer, adaptive equalizer and decision-feedback equalizer [**?**]. However, both linear equalizer and adaptive equalizer do not work well in molecular communication due to time-varying channel response. In this chapter, we utilize the concept of decision feedback and introduce a method to mitigate the effect of ISI.

The rest of this chapter is organized as follows: In Section II, we introduce the settings of a binary QM molecular communication system in details. We also describe the charac-

teristics and the mathematical model of a Brownian motion channel. Section III focuses on deriving the decision rule for one-shot transmission of the binary QM system and extending it to the M-ary transmission case. In Section IV, we consider serial transmission and take ISI effect into account. ISI cancellation method is also described in this section. Numerical results are shown in Section V. Finally, we make conclusions in Section VI.

3.2 System model

In this section, we first give a general model for transmitter, receiver, and channel in molecular communication. We then describe a QM system of M quantity levels (M-ary modulation) bearing $\log_2 M$ information bits, which will be used later to apply our ISI cancellation method.

3.2.1 Transmitter

Fig. 3.1 illustrates a transmitter nano-machine TN transmitting molecules to a receiver nano-machine RN. When TN receives the information (e.g. bit pattern) to be transmitted, it starts storing certain number of molecules in a vesicle (i.e. container that stores molecules) and release these molecules simultaneously into the environment. The number of released molecules differs according to the transmitting information. In practical situations, molecules leaves the vesicle with random timing which is discussed in [**?**]. In this paper, we simply assume that molecules exit the vesicle simultaneously.

3.2.2 Receiver

RN is located at a position $d > 0$ apart from TN. There are several receptors capturing molecules on RN. RN counts the number of molecules it captures and perform detection according to the number. We assume the molecules can be perfectly captured by the receptors and RN does not have counting errors. Furthermore, once a molecule arrives at RN, it will be removed from the communication medium.

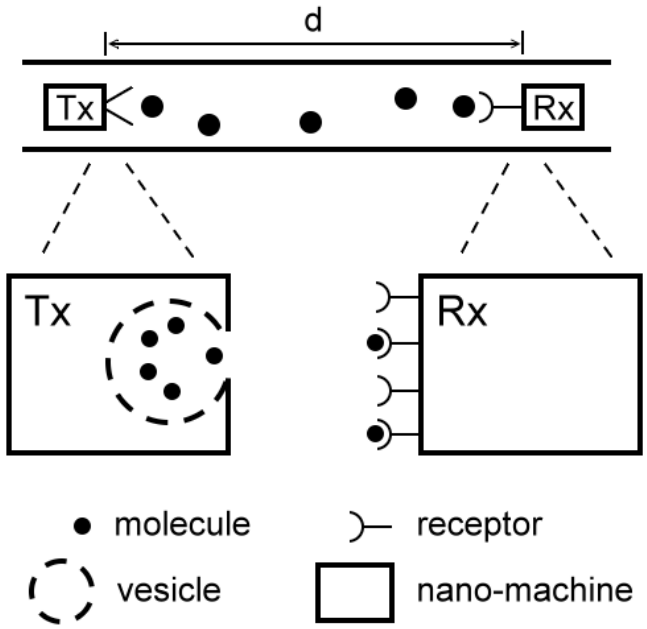

Figure 3.1: Transmission from TN to RN through a fluid medium.

3.2.3 Channel

Consider a fluid medium between TN and RN with positive drift velocity v. The molecules are all constrained to move in a one-dimensional space. We assume that the trajectory of emitted molecules can be modeled with independent Brownian motions [**?**]. Let X denote the random variable representing the first hitting time (i.e. time difference between releasing and capturing) of a molecule. If $v > 0$, it can be shown that the probability density function (pdf) of X is given by the inverse Gaussian (IG) distribution [**?**]

$$f_X(x) = \begin{cases} \sqrt{\dfrac{\lambda}{2\pi x^3}} \exp\left\{-\dfrac{\lambda(x-\mu)^2}{2\mu^2 x}\right\}, & x > 0, \\ 0, & x \leq 0, \end{cases} \tag{3.1}$$

$$\mu = \frac{d}{v} \text{ and } \lambda = \frac{d^2}{2D},$$

where D denotes the diffusion coefficient which is given by

$$D = \frac{k_B T}{6\pi n r}$$

where k_B is the Boltzmann constant, T is the temperature, n is the viscosity of the fluid medium, and r is the radius of molecule. For simplicity, we assume that the radii for all molecules are the same so that the diffusion coefficients are the same.

3.2.4 QM system

Consider a time-slotted M-ary communication with signaling interval T_s, TN can release M different quantities of molecules into the channel. Denote those M quantities by L_m, where $m \in \{0, 1, 2, \cdots, (M-1)\}$. Assume the *a priori* probability for releasing L_m molecules to be q_m. At the starting time of each transmission time slot, L_m molecules are emitted simultaneously from the transmitter to indicate the transmission of a symbol. We assume perfect synchronization between the transmitter and the receiver. During each time slot, RN counts the total number of arriving molecules. An appropriate decision rule, proposed in Section **??**, is then applied to determine the transmitted data bit at the end of each time slot. The molecules which fail to arrive within the corresponding time slot become a source of interference, which will cause performance degradation to the detections of later coming symbols. Fig. 3.2 is an example of QM system with $M = 4$ and uniform quantity levels.

Perfect synchronization between TN and RN is assumed in this chapter, in chapter [ ] we provide a possible realization which is based on sending training molecular impulses and detecting the concentration peaks.

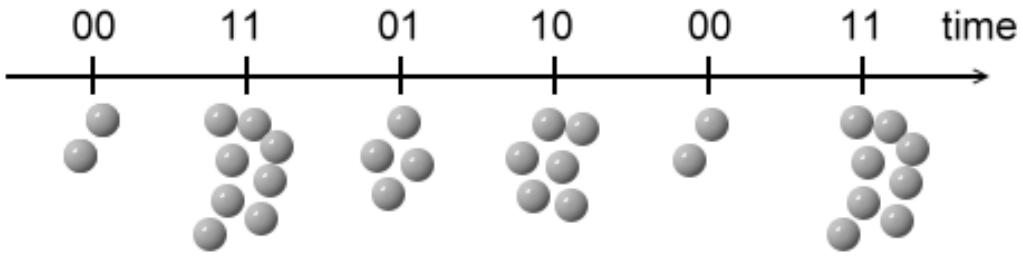

Figure 3.2: Illustration of quantity-based modulation scheme with $L_0 = 2$, $L_1 = 4$, $L_2 = 6$, $L_3 = 8$.

3.3 Detection in one-shot transmission

In this section, we discuss the detection rule of the system for one-shot transmission. The main contribution of our work is that we separate the ISI cancellation problem from the detection to achieve a more flexible and modularized design, which is different from previous works [**?**].

3.3.1 Binary Detection

We define two hypotheses H_0 and H_1. H_0 is the hypothesis that L_0 molecules are transmitted (indicating bit 0), and H_1 is the hypothesis that L_1 molecules are transmitted (indicating bit 1). Denote the conditional pdf of the number of received molecules in a particular time slot, given that hypothesis H_m is true, by $P(N = n|H_m)$, $m \in \{0, 1\}$. Using the inverse Gaussian pdf given in (3.1), we define the probabilities p_j as:

$$p_j = \int_{jTs}^{(j+1)T_s} f_X(x)dx \tag{3.2}$$

for $j \in \{0, 1, \cdots\}$, which is the probability that the traveling time of a molecule falls in the interval $[jT_s, (j + 1)T_s]$, where j is the index of the time slots. Define Y_k to be the indicator random variable showing whether the k-th molecule emitted in a one-shot transmission arrives within T_s given that H_m is true. That is,

$$Y_k = \begin{cases} 1, & \text{if the } k\text{-th molecule arrives within } T_s, \\ \\ 0, & \text{otherwise.} \end{cases} \tag{3.3}$$

Let N be the random variable denoting the total number of molecules arriving at the receiver within a particular time slot. We have the following relation:

$$P(N = n|H_m) = P(Y_1 + Y_2 + ... + Y_{L_m} = n). \tag{3.4}$$

Given the number of the transmitted molecules, N thus follows a binomial distribution with mean and variance as $L_m p_0$ and $L_m p_0(1-p_0)$, respectively. For large L_m, we approximate the binomial distribution by a Gaussian distribution with the knowledge of the mean and variance of N. Since it is difficult to manipulate directly with the binomial pdf, we will derive our detection threshold using Gaussian approximations instead. Namely, we have

$$P(N=n|H_m) \approx \frac{\exp\left\{-\frac{(n-L_m p_0)^2}{2L_m p_0(1-p_0)}\right\}}{\sqrt{2\pi L_m p_0(1-p_0)}}. \tag{3.5}$$

As a special case, the distributions of N under two hypotheses can thus be obtained as

$$P(N=n|H_0) \approx \frac{\exp\left\{-\frac{(n-L_0 p_0)^2}{2L_0 p_0(1-p_0)}\right\}}{\sqrt{2\pi L_0 p_0(1-p_0)}}, \tag{3.6}$$

$$P(N=n|H_1) \approx \frac{\exp\left\{-\frac{(n-L_1 p_0)^2}{2L_1 p_0(1-p_0)}\right\}}{\sqrt{2\pi L_1 p_0(1-p_0)}}. \tag{3.7}$$

According to the conventional hypothesis testing theory [**?**, **?**], the decision rule can be expressed using the likelihood ratio $\Lambda(N)$ as

$$\Lambda(N) = \frac{P(N|H_1)}{P(N|H_0)} \underset{H_0}{\overset{H_1}{\gtrless}} \frac{q_0}{q_1}. \tag{3.8}$$

If we assume equal *a priori* probabilities $q_0 = q_1 = 1/2$, due to the characteristic of Gaussian distribution shown in Fig. 3.3, the decision rule can be further reduced to

$$N \underset{H_0}{\overset{H_1}{\gtrless}} \eta \tag{3.9}$$

for some threshold η, where η is the solution of the following equation:

$$P(N=\eta|H_0) = P(N=\eta|H_1). \tag{3.10}$$

By (3.6) and (3.7), we have

$$\sqrt{\frac{L_1}{L_0}} = \exp\left\{\frac{(L_1 - L_0)(\eta^2 - p_0^2 L_0 L_1)}{2L_0 L_1 p_0(1-p_0)}\right\}. \tag{3.11}$$

Taking logarithms to both sides, the equation becomes

$$\eta = \sqrt{\frac{L_1 L_0 \ln(L_1/L_0)}{L_1 - L_0} p_0(1-p_0) + p_0^2 L_0 L_1}. \tag{3.12}$$

In other words, if the received number of molecules is greater than the threshold η, the receiver will determine H_1 as the hypothesis testing result; otherwise H_0 will be decided.

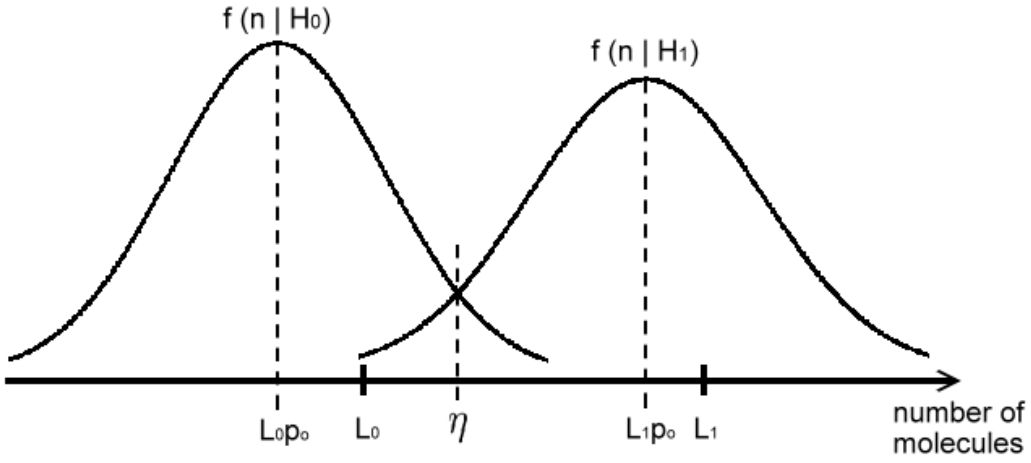

Figure 3.3: Demonstration of the process of finding η in a binary QM system, where f is the conditional pdf of N given H_m is true.

3.3.2 M-ary Detection

The detection rule can be extended to M-ary detection with only a few adjustments. Suppose we have multiple hypotheses H_m where $m \in \{0, 1, 2, \cdots, (M-1)\}$ which represent the transmission of L_m molecules. The goal is to decide which $\hat{m}$ we should choose. The maximum *a priori* (MAP) detection rule is:

$$\hat{m}(N) = \underset{m}{\operatorname{argmax}}\, P(N|H_m). \tag{3.13}$$

Due to the properties of Gaussian distribution, the above MAP detection rule can be simplified to pairwise comparisons between the "neighboring" conditional probability distributions.

To write down the expressions explicitly, we define a set of thresholds $E = \{\eta_j \in [-\infty, \infty] : j = 0, 1, 2, \cdots, M\}$, and let $\eta_0 = -\infty$ and $\eta_M = \infty$. For $j = 1, 2, \cdots, (M-1)$, η_j can be obtained by solving the equations

$$P(N = \eta_j | H_{j-1}) = P(N = \eta_j | H_j). \tag{3.14}$$

With the thresholds determined, the detection rule for M-ary transmission can be expressed as

$$\hat{m}(N) = \sum_{k=0}^{M-1} k \cdot u\left[-(N - \eta_k)(N - \eta_{k+1})\right]. \tag{3.15}$$

where $u(\cdot)$ denotes the unit step function.

3.3.3 Error Rate Analysis

After the construction of the transmission and decision rules, we then analyze how it performs in terms of symbol or bit error rate. Consider a specific case for $M = 2$ and $q_0 = q_1 = 1/2$. Denote the false alarm probability as P_F and the missing probability as P_M. The error rate can be written as

$$P_e = q_0 P_F + q_1 P_M = \frac{1}{2}(P_F + P_M). \tag{3.16}$$

From Fig. 3.3 and the decision rule derived in Subsection A, it can be shown that

$$P_F = P(N > \eta | H_0) = Q\left(\frac{\eta - L_0 p_0}{\sqrt{L_0 p_0 (1 - p_0)}}\right), \tag{3.17}$$

$$P_M = P(N < \eta | H_1) = Q\left(\frac{L_1 p_0 - \eta}{\sqrt{L_1 p_0 (1 - p_0)}}\right), \tag{3.18}$$

where $Q(\cdot)$ denotes the Q-function. By substituting (3.12) into equation (3.17) and (3.18), we can evaluate the error rate P_e in (3.16). Fig. 3.4 shows the comparison between our analysis and numerical results.

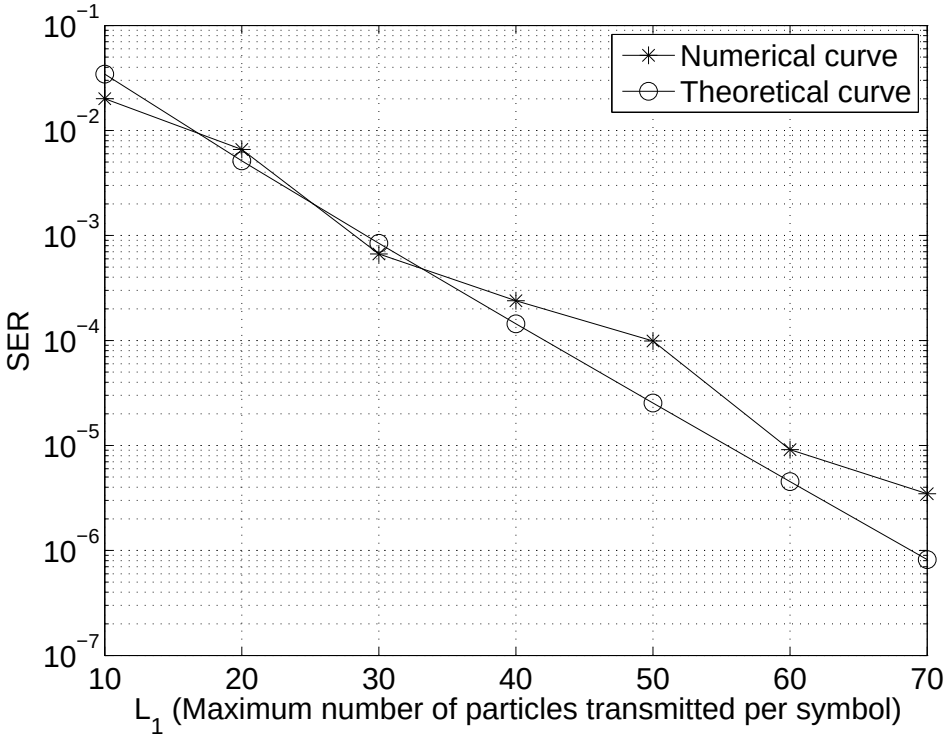

Figure 3.4: Theoretical result versus numerical result for one-shot binary quantity-based modulation.

3.4 Serial transmision and ISI cancellation

The above described QM molecular communication system seems to work already. However, in practical situations, we need to perform serial transmissions rather than one-shot transmission. Thus the ISI effect must be taken into account. Our results show that if we do not modify our one-shot detection rule, the system performance will fall dramatically under serial transmission environments due to the severe ISI effect. To solve this problem, we propose a method to mitigate the ISI effect.

In order to mitigate the ISI effect, we first need an estimation of the number of the delayed molecules that come from former time slots. If we know the conditional probability distribution of the number of ISI molecules conditioned on the current received number,

then we can estimate the ISI effect as the conditional mean. However, the conditional distribution does not have a closed-form solution for inverse Gaussian random variables. Here we proposed another intuitive way to do this estimation.

First, we define "memory-Γ cancellation" to mean that the ISI effect during the past Γ time slots are taken into account when making decision. We first use memory-1 cancellation as a demonstrative example. Suppose that the traveling time τ of each molecule can be described using an inverse Gaussian random variable with cumulative distribution function (cdf) $F_\tau(t) = \int_0^t f_X(x)dx$. Our proposed ISI cancellation method is: if the number of molecules received during the $(i-1)$-th time slot is n_{i-1} and the decided transmission quantity level is $\hat{l}_{i-1}$, where $\hat{l}_{i-1} \in \{L_0, L_1, \cdots, L_{M-1}\}$, we then subtract $\hat{l}_{i-1} \cdot [F_\tau(2T_s) - F_\tau(T_s)]$ (the *a priori* expected received number in the i-th time slot from the $(i-1)$-th time slot) from n_i before making the i-th decision. In other words, the actual number $\tilde{n}_i$ used in making decision is

$$\tilde{n}_i = n_i - \hat{l}_{i-1} \cdot [F_\tau(2T_s) - F_\tau(T_s)]. \tag{3.19}$$

Likewise, we can perform memory-Γ cancellation if we have enough buffer at the receiver end to memorize temporarily the recently received numbers of molecules. More explicitly, denote the probabilities that a single transmitted molecule arrives during the time interval $[jT_s, (j+1)T_s]$ by p_j for $j \in \mathbb{N} \cup \{0\}$ as before. If the decided transmission quantity level of the current time slot is $\hat{l}$, where $\hat{l} \in \{L_0, L_1, \cdots, L_{M-1}\}$, then the received number of molecules j time slots later should be subtracted by $\hat{l} \cdot p_{j+1}$ before making decision. In other words, if the number of molecules received in i-th time slot is n_i, the actual number $\tilde{n}_i$ used in making decision is

$$\tilde{n}_i = n_i - \sum_{j=1}^{\Gamma} \hat{l}_{i-j} p_{j+1}. \tag{3.20}$$

For binary QM systems, the decision rule can be written as

$$\tilde{n}_i = n_i - \sum_{j=1}^{\Gamma} \hat{l}_{i-j} p_{j+1} \underset{H_0}{\overset{H_1}{\gtrless}} \eta. \tag{3.21}$$

The extension to M-ary QM systems is straightforward.

3.5 Numerical results

In this section, we first discuss the binary and M-ary QM modulation systems with and without performing ISI cancellation. After that, we make comparisons of the system performance under different time slot durations.

The number of molecules is one of the main resources utilized in molecular communications. Analogous to the "power" concept in conventional communications, we need to take this number into account when comparing the system performances. In the following subsections, we present the results under different maximum number of molecules allowed per symbol, and the quantity levels are uniformly spaced. The simulation parameters are $d = 0.2\ cm$, drift velocity $v = 0.01\ cm/s$, diffusion coefficient $D = 0.05\ cm^2/s$, and time slot duration $T_s = 5\ s$.

3.5.1 SER comparison with and without ISI cancellation

In Fig. 3.5, a binary transmission system with memory-1 and memory-2 cancellaion is considered. The SER drops from 0.04 to 0.01 when $L_1 = 30$, and drops from 10^{-2} to 10^{-4} when $L_1 = 90$. The improvement grows as L_1 increases, which means that by choosing L_1 properly, a reliable end-to-end transmission can be achieved. We also observe that even without ISI cancellation, the error rate will drop as L_1 increases. The reason is that the spacing between symbols is increased. However, as shown in Fig. 3.6, it is not the case for the quaternary transmission system. It can be seen that even though L_3 becomes large, the error rate is still high without ISI cancellation, which means we cannot rely solely on increasing the maximum number of molecules without ISI cancellation.

It is worth mentioning that the ISI cancellation method can be performed not only in such quantity-based modulation systems, but it can also be used in other systems like on-off keying[1] with slight modifications.

[1] Transmitting zero or a single molecule.

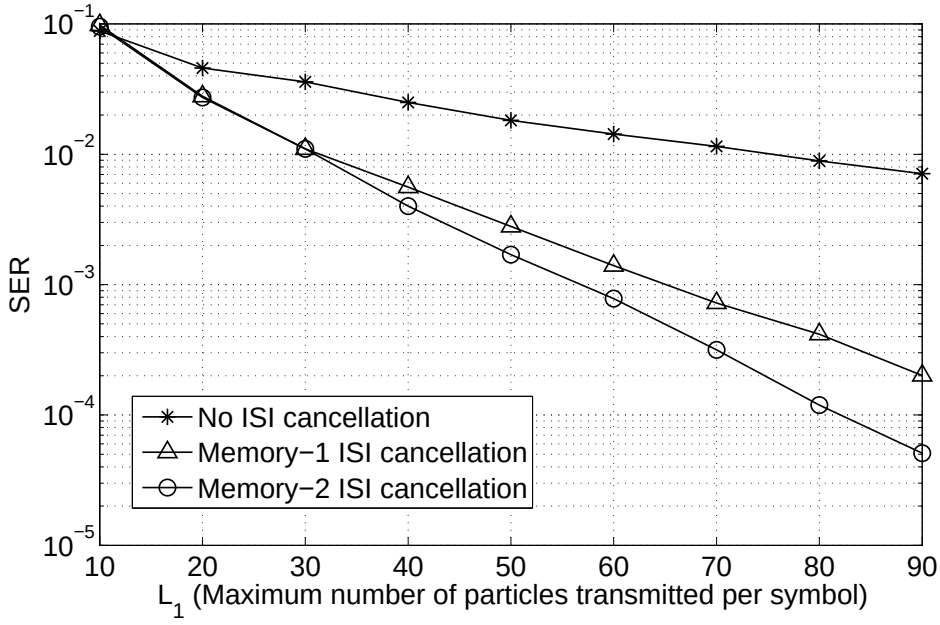

Figure 3.5: Binary quantity-based modulation with ISI cancellation.

3.5.2 Performance Under Different Duration of Time Slot

In this subsection, we consider a binary transmission system with and without ISI cancellation for different time slot durations. From Fig. 3.7, we can observe that the SER decreases as the duration T_s increases. In other words, to improve performance, one can increase the duration of the time slot as shown in Fig. **??**. Although the error rate is already quite acceptable, it can be further improved by the ISI cancellation approach. The improvements is about 10 times better when $T_s = 10\ s$ and $L_1 = 70$. Note that when T_s is small, say $T_s = 1\ s$, compared to the expected first-hitting time d/v, the error rate increases even if we increase L_1 when no cancellation is performed. This is because when T_s is small, molecules tend not to arrive in one symbol time but stay in the background, and that a larger L_1 will cause a larger amount of molecules to be in the background and hence larger interference.

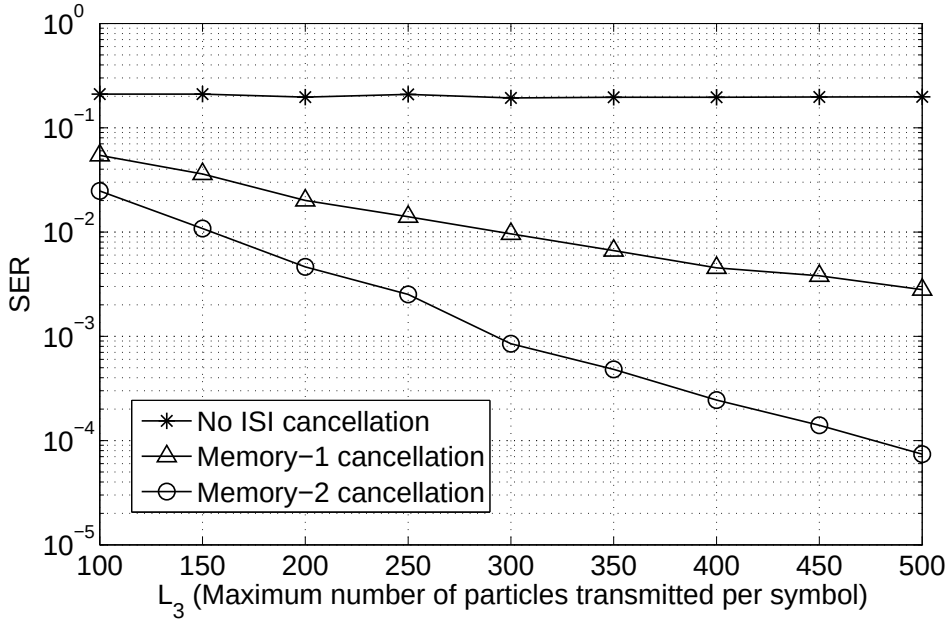

Figure 3.6: Quaternary quantity-based modulation with ISI cancellation.

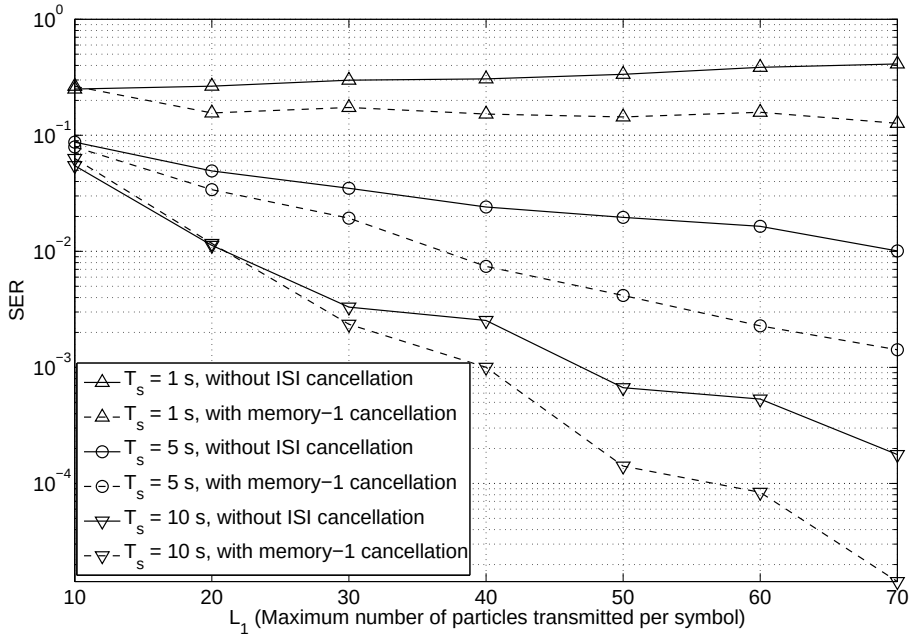

Figure 3.7: Binary quantity-based modulation with ISI cancellation under different T_s.

Chapter 4

Theory of surface plasmon polaritons in metallic nano-structures

4.1 Definition of plasmon

Plasmon is collective oscillation of conduction electron gas, a quasi-particle resulting from the quantization of plasma oscillations just like phonons are quantizations of mechanical vibrations. The simplest case is the volume plasmon as shown in Figure 4.1. We

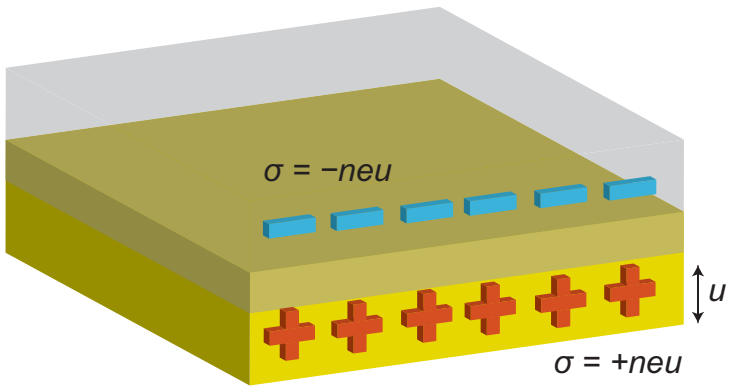

Figure 4.1: Longitudinal collective oscillations of the conduction electrons of a metal (Volume plasmons)

can derive plasma frequency ω_p from the simple harmonics oscillation model, a collective displacement of the electron cloud by a distance u leads to a surface charge density $\sigma = \pm neu$ at the slab boundaries. This establishes a homogeneous electric field $\mathbf{E} = \frac{neu}{\varepsilon_0}$ inside the slab. Thus, the displaced electrons experience a restoring force, and their move-

ment can be described by the equation of motion $nm\ddot{u} = -ne\mathbf{E}$. Inserting the expression for the electric field, this leads to

$$nm\ddot{u} = -\frac{n^2e^2u}{\varepsilon_0} \tag{4.1a}$$

$$\ddot{u} + {\omega_p}^2 u = 0. \tag{4.1b}$$

The plasma frequency $\omega_p = \sqrt{\frac{ne^2}{\varepsilon_0 m}}$ can thus be recognized as the natural frequency of a free oscillation of the electron sea. The quanta of these charge oscillations are called plasmons. Due to the longitudinal nature of the excitation, volume plasmons do not couple to transverse electromagnetic waves, and can only be excited by particle impact. We can derive the dispersion relation of the generalization of volume plasmons, traveling plasma waves, from curl electric field equations (Equations 4.2a)

$$\boldsymbol{\nabla} \times \boldsymbol{\nabla} \times \mathbf{E} = -\mu_0 \frac{\partial^2 \mathbf{D}}{\partial t^2} \tag{4.2a}$$

$$\mathbf{K}(\mathbf{K} \cdot \mathbf{E} - K^2\mathbf{E}) = -\varepsilon(\mathbf{K}, \omega)\frac{\omega^2}{c^2}\mathbf{E} \tag{4.2b}$$

and plasma model, and a simple equation of motion for an electron of the plasma subjected to an external electric field $\mathbf{E}$

$$m\ddot{\mathbf{x}} + m\gamma\dot{\mathbf{x}} = -e\mathbf{E}. \tag{4.3}$$

Assuming a harmonic time dependence $\mathbf{E}(t) = \mathbf{E}_0 \mathrm{e}^{-i\omega t}$ of the driving field, a particular solution of this equation describing the oscillation of the electron is $\mathbf{x}(t) = \mathbf{x}_0 \mathrm{e}^{-i\omega t}$. The complex amplitude $\mathbf{x}_0$ incorporates any phase shifts between driving field and response via

$$\mathbf{x}(t) = \frac{e}{m(\omega^2 + i\gamma\omega)}\mathbf{E}(t). \tag{4.4}$$

The displaced electrons contribute to the macroscopic polarization

$$\mathbf{P} = -\frac{ne^2}{m(\omega^2 + i\gamma\omega)}\mathbf{E}(t). \tag{4.5}$$

Inserting $\mathbf{P}$ into dielectric displacement field equation $\mathbf{D} = \varepsilon_0\mathbf{E} + \mathbf{P}$ yields

$$\mathbf{D} = \varepsilon_0(1 - \frac{\omega_p^2}{\omega^2 + i\gamma\omega})\mathbf{E}, \tag{4.6}$$

where $\omega_p^2 = \frac{ne^2}{\varepsilon_0 m}$. Therefore, the dielectric function of the free electron gas

$$\varepsilon(\omega) = 1 - \frac{\omega_p^2}{\omega^2 + i\gamma\omega}. \tag{4.7}$$

We arrive at the desired result by using equation 4.7 and the generic dispersion relation $K^2 = \varepsilon(\mathbf{K}, \omega)\frac{\omega^2}{c^2}$, the dispersion relation of traveling waves becomes

$$\omega^2 = \omega_p^2 + \mathbf{K}^2c^2. \tag{4.8}$$

From this relation, we can figure out the oscillation properties in any frequency of external field. Note that this branch can not confine the electromagnetic waves, it would radiate out the energy, so this mode is also called radiative surface plasmon.

4.2 Surface plasmon polaritons at interface between dielectric and metal

Surface plasmon polaritons (SPPs) are eigenmodes of transverse magnetic (TM) waves, which coupling the electromagnetic fields to oscillations of the conductor's electron plasma, propagate at a interface between dielectric and metal, and are confined in perpendicular direction. Providing a flat interface between dielectric and metal half-spaces with dielectric constants ε_d and ε_m , respectively, and assuming the interface normal to z direction and the SPPs propagate along the x direction, the SPP wave vector β is related to the frequency ω through the dispersion relation

$$\beta = k_0\sqrt{\frac{\varepsilon_d\varepsilon_m}{\varepsilon_d + \varepsilon_m}}, \tag{4.9}$$

where $k_0 = \omega/c$ is the free-space wave vector. We take ω to be real and allow β to be complex.

The optical response of metals is often described by the Drude model for a free-electron gas [2],

$$\varepsilon_{Drude}(\omega) = 1 - \frac{\omega_p^2}{\omega^2 + i\Gamma\omega}, \tag{4.10}$$

in which Γ is a damping rate due to electron-electron and electron-phonon scattering. Figure 4.2 shows the dispersion curve 4.9 with Drude metal in the absence of losses ($\Gamma = 0$) for air ($\varepsilon_d = 1$) and fused silica ($\varepsilon_d = 2.25$) interface. For small wave vectors SPPs

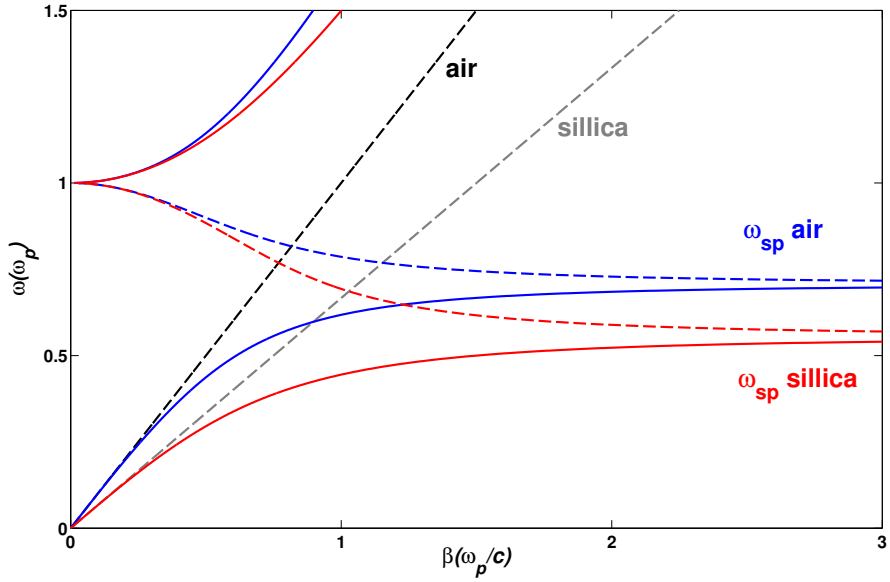

Figure 4.2: Dispersion relation of SPPs at the interface between a Drude metal with negligible collision frequency and air (blue curves) and silica (red curves).

propagation constant β is close to k_0 at the light line, in the opposite regime of the frequency close to surface plasmon frequency ω_p. It also shows that the SPPs line lying to the right of the respective light lines of air and silica, so that SPPs are directed by light due to phase mismatching. The wave vector mismatch between SPPs and radiation modes needs to be overcome in order to excite or detect SPPs. This can be achieved by multiple methods [3]. In the Otto configuration, light in a prism that is brought in close vicinity to a metal surface can excite SPPs through coupling to the evanescent field. Because light in the prism has a larger wave vector than that in air, it can be phase-matched to the SPPs. In the related Kretschmann-Raether geometry, coupling to SPPs occurs through a metal film

that is deposited on a prism. In the grating coupling configuration, metal surface with a shallow grating of grooves or holes with lattice constant a. For the simple 1D grating of grooves depicted in Figure 4.3, phase-matching takes place when the condition is fulfilled

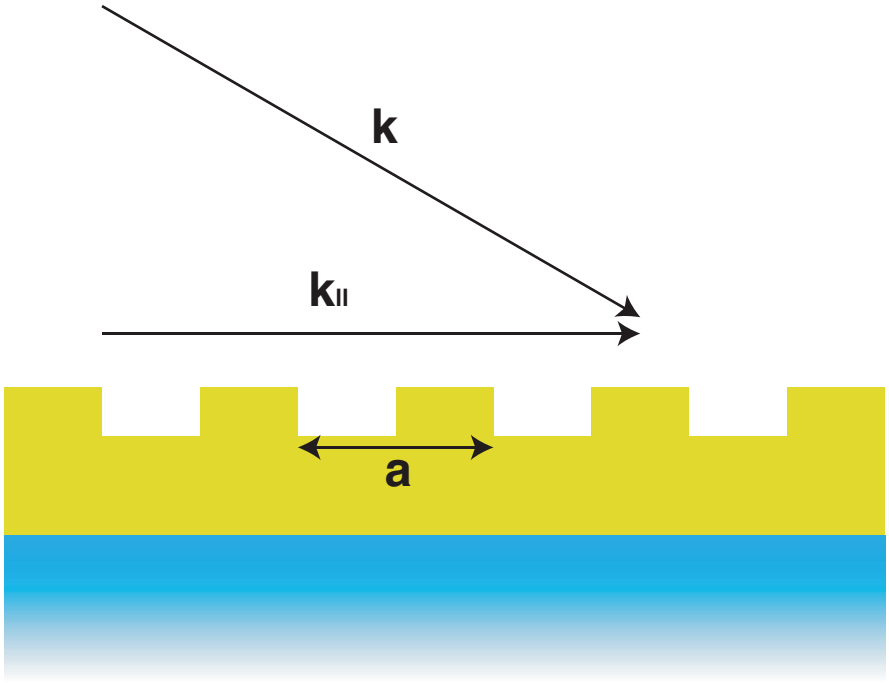

Figure 4.3: Phase-matching of light to SPPs the grating coupling configuration.

$$\beta = k_0 \sin\theta \pm \nu g, \tag{4.11}$$

where $g = \frac{2\pi}{a}$ is the reciprocal vector of the grating, and $\nu = (1, 2, 3 \dots)$. As with prism coupling, excitation of SPPs is detected as a minimum in the reflected light. The reverse process can also take place, SPPs propagating along a surface modulated with a grating can couple to light and thus radiate.

Chapter 5

Experiment

5.1 Atomic force microscopy

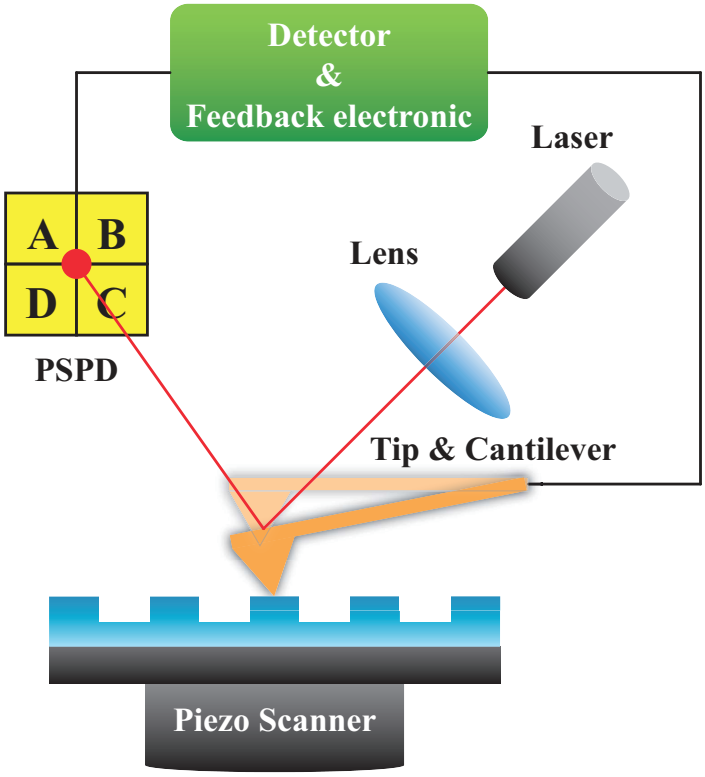

Figure 5.1: Schematic of atomic force microscopy.

Atomic force microscope (AFM) is a type of scanning probe microscopes (SPM) [4]. The schematic of AFM is shown in Figure 5.1. AFM operates by measuring force between a probe and the specimen surfaces. In general, the probe is a sharp tip at a cantilever's end. The cantilever can be deflected by atomic forces to sufficiently large amount, then AFM

can measure the vertical and lateral deflections of the cantilever by using the optical system. A laser beam is transmitted to cantilever, and the reflected laser beam is detected with a position-sensitive photo detector (PSPD). PSPD is four-sectional that allows measuring not only vertical but lateral bending too(Figure 5.2). The output of the PSPD is provided to a computer for processing of the data for providing a topographical image of the surface with atomic resolution, and controlling the height between probe and specimen surfaces by applying voltage on piezoelectric scanner.

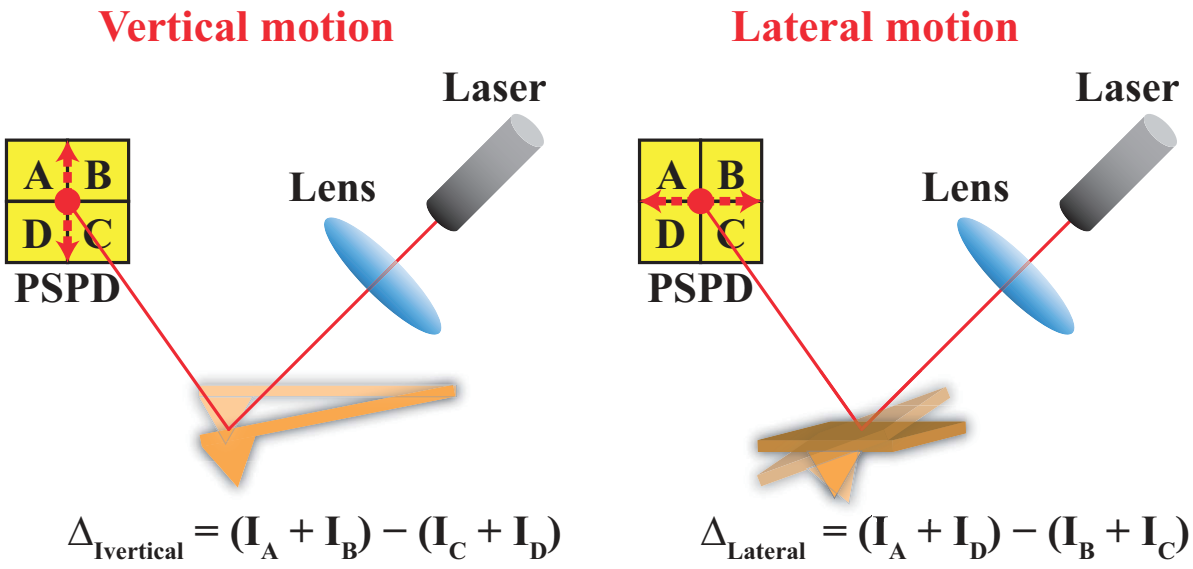

Figure 5.2: Schematic of optical system for cantilever deflections detection.

The physical principle of the AFM operation is based on interaction between the probe tip and the specimen surface(Figure 5.3). When the cantilever approaches the specimen surface, Van der Waals forces start acting upon it . They are sufficiently far-ranging and are felt at the distance of a few tens of angstroms. Then at the distance of several angstroms repulsive force starts acting. In humid air a water layer is present on the specimen surface. The capillary force arises that holds the tip in contact with the surface and increases the minimum achievable interaction force. Electrostatic interaction between the probe and the sample may appear rather often. This can be both attraction and repulsion. Van der Waals attraction forces, capillary, electrostatic and repulsion forces at the point where the tip touches the sample and forces acting upon the tip from the deformed cantilever compensate each other in equilibrium. Based on the type and degree of this interaction

the AFM modes can be broken down into contact and semi-contact(Figure 5.3), which is a transition mode between the contact and non-contact modes.

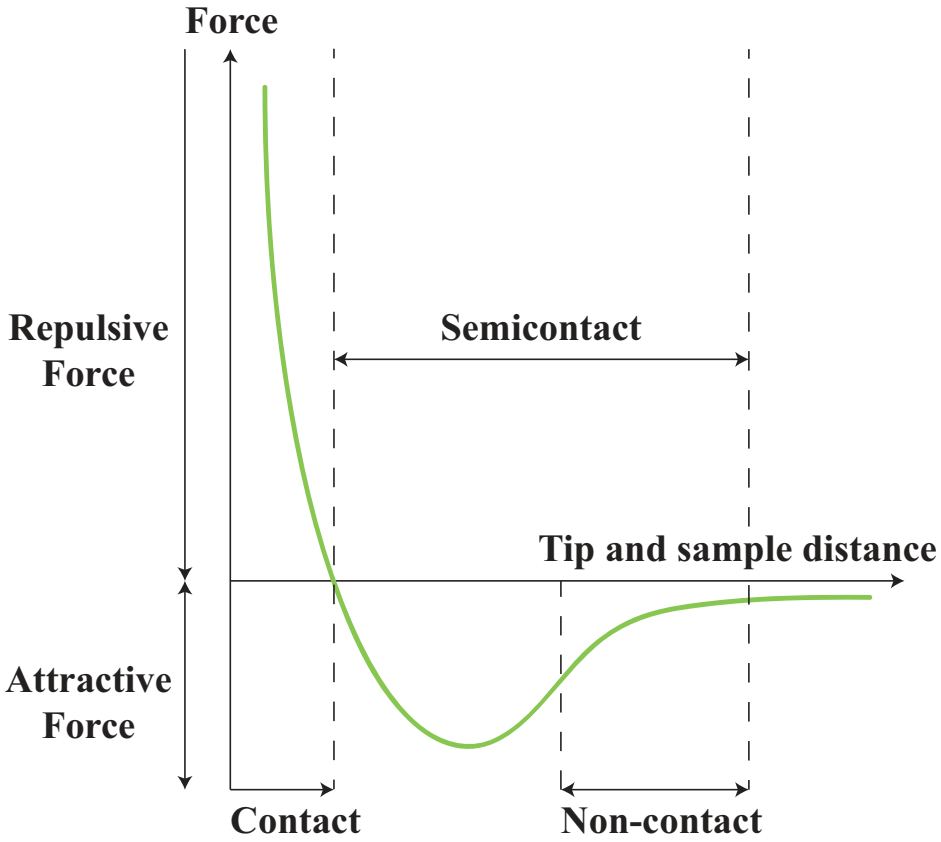

Figure 5.3: Sketch of tip-sample forces.

Contact mode In contact mode of operation the cantilever deflection under scanning reflects repulsive force acting upon the tip. Repulsion force $\mathbf{F}$ acting upon the tip is related to the cantilever deflection value $\mathbf{x}$ under Hooke's law: $\mathbf{F} = -K \cdot \mathbf{x}$, where K is cantilever spring constant. The spring constant values for different cantilevers usually vary from 0.01 to several $\mathbf{N/m}$.

In our units the vertical cantilever deflection value is measured by means of the optical registration system and converted into electrical signal DFL (difference signal between the upper and lower halves of the PSPD) . In contact mode the DFL signal is used as a parameter characterizing the interaction force between the tip and the surface. There is a linear relationship between the DFL value and the force. In constant force mode of operation the deflection of the cantilever is maintained by the feedback circuitry on the

preset value. So vertical displacement of the scanner under scanning reflects topography of sample under investigation.

Contact force microscopy is surface topography measurement in the contact mode.The microscope operation in the mode of maintaining constant interaction force between the tip and the surface sample, and is the base for measuring surface topography as well as for measuring local rigidity, local viscosity and local friction force. Constant force mode has some advantages and disadvantages. Main advantage of constant force mode is possible to measure with high resolution simultaneously with topography and some other characteristics, such as friction forces, spreading resistance etc. Constant force mode has also some disadvantages. Speed of scanning is restricted by the response time of feedback system. When exploring soft samples they can be destroyed by the scratching because the probe scanning tip is in direct contact with the surface. Therefore, under scanning soft unhomogeneous samples the local flexure of sample surface varies. As a result acquired topography of the sample can be proved distorted. Possible existence of substantial capillary forces imposed by a liquid adsorption layer can decrease the resolution.

Semi-contact mode The semi-contac mode can be characterized by some advantages in comparison with contact mode. First of all, in this mode the force of pressure of the cantilever onto the surface is less, that allows to work with softer materials such as polymers and bio-organics. The semi contact mode is also more sensitive to the interaction with the surface that gives a possibility to investigate some characteristics of the surface distribution of magnetic and electric domains, elasticity and viscosity of the surface.

Widely used semi-contact mode has some disadvantage concerned with the usage of the feedback circuit. The scanning speed in semi-contact mode is restricted by the feedback circuit reaction time. This disadvantage can be overcome by the fact that under scanning new value of cantilever oscillation amplitude (and error signal) usually is achieved faster than preset value of the cantilever oscillation amplitude can be reached by the feedback system. Time of the reaching new value of the oscillation amplitude is determined by the oscillation period and Q-quality of the cantilever. The feedback error signal, emerging when scanning in the semi-contact mode, contains some additional information about the

topography. It can be utilized for achieving a more precise recovery of the relief.

Additionally, similarly to the contact error mode, which can be considered as intermediate between the constant force mode and constant height mode, the feedback gain factor (i.e. the feedback processing speed) can be adjusted for the system to be able to trace subtle changes of the relief and to be too slow to trace the steep changes. Then, when the probe travels over minor irregularities, scanning will be carried out with an almost constant piezo scanner length. As a result, the slow changes of the relief will hardly show up on the images, and the steep changes will appear in high contrast. This may be helpful in finding minor irregularities on large areas against major sloping relief features. It must be noted that height of the minor irregularities must be less than amplitude of cantilever oscillation.

5.2 Scanning electron microscopy

The scanning electron microscope (SEM) is used for the observation of specimen surfaces [5]. When the specimen is irradiated with a fine electron beam, secondary electrons are emitted from the specimen surface. Topography of the surface can be observed by two-dimensional scanning of the electron probe over the surface and acquisition of an image from the detected secondary electrons. The concept schematic of commercial SEM (JEOL, JSM-6500F) is shown in Figure 5.4. The basic unit is composed of an electron optical system, a specimen stage, a secondary-electron detector, an image display unit, and an operation system. The electron optical system consists of an electron gun, a condenser lens and an objective lens to produce an electron probe, a scanning coil to scan the electron probe, and other components. The system inside of the microscope column are kept at vacuum.

The JSM-6500F utilizes a Schottky type field-emission (T-FE) gun for the electron source. The T-FE gun can constantly supply the surface of the cathode with zirconium oxide by heating the surface of cathode to 1800 K. For this reason, it can easily obtain stable and high probe current (range from several pA to 100 nA) compared with the traditional thermal emission electron gun and cold field-emission gun.

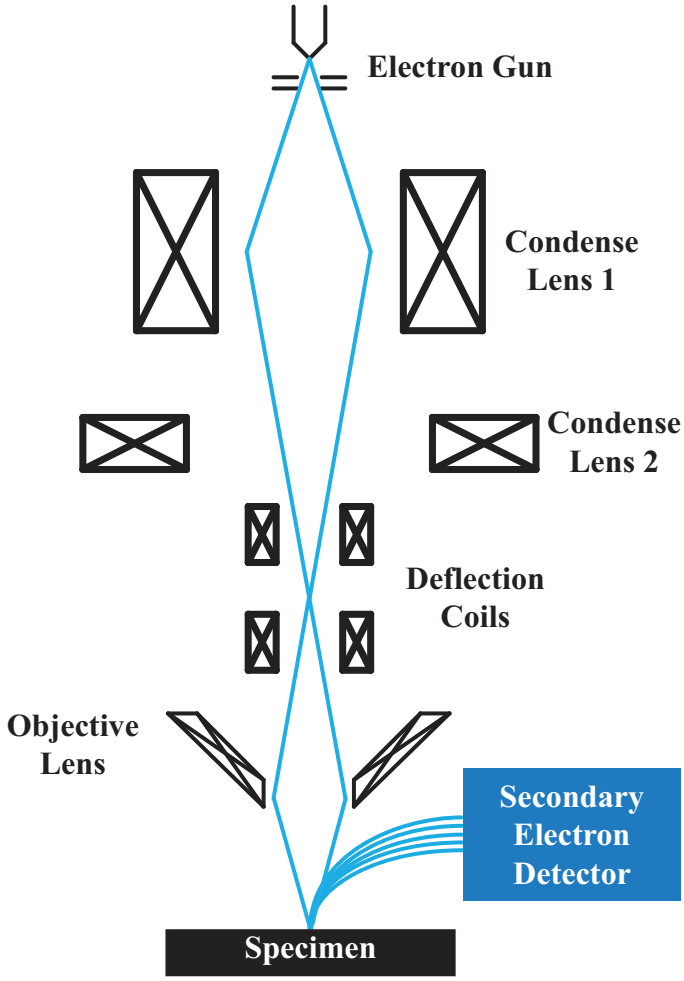

Figure 5.4: Basic construction of a scanning electron microscopy.

The magnetic condenser and objective lens system act to control the diameter of the beam as well as to focus the beam on the specimen due to a rotationally-symmetric magnetic field is formed when we pass a direct electric current through a coilwound electric wire in the magnetic lens. A pair of deflector coils, which between the condenser and objective lens, controlled by the scan generator, which are responsible for rastering that focused beam across the specimen surface. The size of the rastering pattern is under magnification control. The beam is rastered from left to right and top to bottom. There is a one-to-one correspondence between the rastering pattern on the specimen and the rastering pattern used to produce the image on the monitor. The resolution we choose to image at will obviously affect the number of pixels per row as well as the number of rows that constitute the scanned area.

The signal is generated from the specimen, and collected by the detector and subse-

quently processed to generate the image. That processing takes the intensity of the signal coming from a pixel on the specimen and converts it to a grayscale value of the corresponding monitor pixel. The monitor image is a two dimensional rastered pattern of grayscale values.

With the beam focused on the specimen surface, all we need to do to change magnification is to change the size of the rastered area on the specimen. The size of the monitor raster pattern is constant. Magnification will increase if we reduce the size of the area scanned on the specimen.

Bibliography

[1] S.A. Maier. *Plasmonics: fundamentals and applications*. Springer Verlag, 2007.

[2] C. Kittel and P. McEuen. *Introduction to solid state physics*, volume 7. Wiley New York, 1976.

[3] H. Raether. *Surface plasmons*. Springer-Verlag Berlin, 1988.

[4] G.K. Bennig. Atomic force microscope and method for imaging surfaces with atomic resolution, February 9 1988. US Patent 4,724,318.

[5] M. Von Ardenne. Das elektronen-rastermikroskop. *Zeitschrift für Physik A Hadrons and Nuclei*, 109(9):553–572, 1938.